Recent Advances in 2D Material-Mediated Immuno-Combined Cancer Therapy

Baojin Ma, Alberto Bianco

Recent Advances in Two-dimensional Material-Mediated Immuno-Combined Cancer Therapy

Baojin Ma,* Alberto Bianco*

Dr. B. Ma

School and Hospital of Stomatology, Cheeloo College of Medicine, Shandong University & Shandong Key Laboratory of Oral Tissue Regeneration & Shandong Engineering Laboratory for Dental Materials and Oral Tissue Regeneration, Jinan, Shandong, 250012, China

Dr. A. Bianco

CNRS, Immunology, Immunopathology and Therapeutic Chemistry, UPR3572, University of Strasbourg, ISIS, 67000 Strasbourg, France

EMAIL: a.bianco@ibmc-cnrs.unistra.fr; baojinma@sdu.edu.cn

Abstract

In the last years, cancer immunotherapy started to attract a lot of attention, becoming one of the alternatives in clinical treatment of cancer. Indeed, one of the advantages of immunotherapy is that both primary and distant tumors can be efficiently eradicated through a triggered immune response. Due to their large specific surface area and unique physicochemical properties, two-dimensional (2D) materials have become popular in cancer immunotherapy, especially as efficient drug carriers. They have been also exploited as photothermal platforms, chemodynamic agents and photosensitizers to further enhance the efficacy of the therapy. In this review, we will focus on the recent development of 2D materials as new tools to combine immunotherapy with chemotherapy, photothermal therapy, photodynamic therapy, chemodynamic therapy, radiotherapy, and radiodynamic therapy. These innovative synergistic approaches intend to go beyond the classical strategies based on a simple delivery function of immune modulators by nanomaterials. Furthermore, the effects of the 2D materials themselves and their surface properties (e.g., chemical modification and protein corona formation) on the induction of an immune response will be also discussed.

Keywords

2D materials; multifunctional materials; surface chemistry; biomedical applications; immune system

1. Introduction

Due to their unique physicochemical properties, various two-dimensional (2D) materials have been widely applied in the biomedical field, for applications in cancer therapy, tissue engineering, biosensing and others.[1, 2] Especially for cancer treatment, 2D materials have attracted a lot of attention. The currently popular 2D materials include graphene materials, 2D Xenes, 2D MXenes, transition metal dichalcogenides, transition metal oxides, 2D metal-organic frameworks, and 2D metal carbides or nitrides.[3-8] Based on their different properties, such 2D materials could be used as efficient means for drug delivery, photothermal therapy (PTT, which utilizes photothermal agents to convert light energy into hyperthermia, leading to the thermal ablation of cancer cells), photodynamic therapy (PDT, which uses photosensitisers to transfer photon energy into reactive oxygen species, provoking cancer cell death), chemodynamic therapy (CDT, which is based on Fenton or Fenton-like reactions to convert H_2O_2 into hydroxyl radicals triggering apoptosis and inhibiting tumor growth), radiotherapy (RT, which uses high-dose radiation to kill cancer cells and eliminate tumors), radiodynamic therapy (RDT, which utilizes ionizing radiation to excite photosensitizers to generate $^1O_2$ against cancer) and specific combination thereof.[8-10]

In the years, cancer immunotherapy gets an exceptional growing progress, especially after ipilimumab obtained the approval from FDA.[11] Ipilimumab is a monoclonal antibody directed towards cytotoxic T-lymphocyte-associated protein 4 (CTLA4) showing a significant increase in the survival of patients with metastatic melanoma. It is well known that cancer immunotherapy is based on immune system activation to target and eradicate cancer cells with durable antitumor responses and less metastasis and recurrence than other therapeutic strategies.[12, 13] Immune biochemical factors, vaccines, checkpoint inhibitors, monoclonal antibodies and other molecules have been widely utilized as efficient modulators to activate the immune system. Checkpoint blockade immunotherapy is a recently developed strategy based on the use of checkpoint inhibitors to arrest the immunosuppressive pathways promoting antitumor T cell activation and maintaining the antitumor T cell effector function.[14, 15] However, the cancer immunotherapy efficiency is still not satisfactory. Indeed, the overall patient response rates are usually below 40% by checkpoint inhibitor therapy.[16] Meanwhile, immunotherapy can trigger mild to serious side effects, such as nausea, vomiting, lung/skin/gastrointestinal/renal toxicities, hypothyroidism, arthralgia, vasculitis, autoimmune hepatitis and other dysfunctions.[17, 18]

To reduce or to overcome the side effects caused by immunotherapy, and further enhance its efficiency, 2D materials provide incomparable advantages, including high specific surface area, biocompatibility, chemical surface modification, targeting possibility, tumor accumulation and unique physicochemical functions.[7, 8, 19, 20] These advantages not only endow 2D materials with efficient delivery capacity and high safety profile but also provide the basis for a variety of immuno-combined cancer therapies. Although the carrier function of 2D materials can improve anticancer efficiency and reduce the drug side effects to a certain degree, an immune cancer therapy depending solely on delivery still scarcely meets patients' expectations and needs. Therefore, the combination of immune therapy with other therapeutic modalities has been put forward as a new

strategy to cure cancer. At present, the combination modes between immunotherapy and other 2D material-based cancer therapeutic methods mainly includes immunotherapy/chemotherapy, immunotherapy/CDT, immunotherapy/PTT, immunotherapy/PDT, immunotherapy/PDT/PTT, immunotherapy/PDT/CDT, immunotherapy/RT, immunotherapy/RDT, immunotherapy/RT/RDT, immunotherapy/chemotherapy/PDT, and immunotherapy/chemotherapy/PDT/PTT. The different combination modes basically depend on the functions of corresponding 2D materials. More cancer cells are destroyed by 2D material-mediated therapies, triggering the release of a large number of antigens and inducing a strong immune response. For example, through antigen presenting dendritic cells (DCs), more $CD8^+$ and $CD4^+$ T cells are generated, leading to a stronger immunotherapy.[21]

This review is aimed to cover the design of 2D material-mediated immune combined cancer therapy and to understand the synergistic effect and the interactions between the immune response and the other therapeutic strategies, unlikely other available reviews that focus mainly on the delivery aspects of nanoparticles and nanomaterials.[22-26] Furthermore, the intrinsic effects of 2D materials and surface properties (such as surface modification and protein corona) on immune response are also described as evaluation criterion to choose the most suitable 2D materials for immune cancer therapy.

2. 2D Materials and Combined Therapies

This section is divided into the different 2D material-mediated immune combined cancer therapies, underlining the combination modes, the therapeutic efficiency, and the interactions between different therapies. The description of the physicochemical characteristics, the essential functions of each material will be presented. Further, the intrinsic immune response of the materials and the effects of protein corona will be also addressed.

2.1. Graphene Family Materials

Graphene family materials (GFMs, such as graphene, graphene oxide/GO, reduced graphene oxide/rGO, and graphene quantum dots/GQDs) are the widest applied 2D materials in nanomedicine due to their unique physicochemical properties and high biocompatibility.[5, 27-29] GO and GQDs are frequently explored in combined therapies because of their high water dispersibility. Chemically modified rGO is instead mainly used for PTT due to the higher photothermal efficiency than GO and the easier preparation than graphene. Generally, GFMs can be considered ideal carriers for drugs and immune regulators. For instance, GO and rGO have been used as potential vaccine adjuvants to improve the antigen immunogenicity for better cancer treatment.[30-32] In addition, GO-templated antibody nanoclusters could activate human natural killer cells for immunotherapy.[33] To further enhance the therapeutic efficiency, GFMs have been transformed into multifunctional platforms for combined cancer therapy. Polyethylene glycol (PEG) and polyethylenimine (PEI) dual-functionalized GO (GO-PEG-PEI) was designed as a carrier for light-controllable CpG oligodeoxynucleotide (ODN) delivery. The photothermally induced local heating

under NIR light irradiation accelerated the intracellular trafficking of the system by increasing cell membrane permeability, resulting in a remarkable enhanced immunostimulation. By a synergistic photothermal and immunological effect, GO-PEG-PEI/CpG complex allowed to cure cancer in a mouse model.[34] Inversely, CpG ODN treatment alone almost had no tumor suppression and the simple delivery effect of GO-PEG-PEI could only improve the therapy efficacy of CpG ODN to a certain not satisfactory extent. It is well known that the pro-inflammatory macrophage M1 phenotype polarization rather than anti-inflammatory M2 phenotype can be beneficial to cancer therapy.[35] Interestingly, PEG-GO-mediated photothermal effect inhibited interleukin-4-induced M2 polarization of macrophages and modulated their antitumor capability.[36] After NIR irradiation, the invasion and migration ability of tumor cells were efficiently supressed by regulating macrophage polarization, leading to a high anti-tumor effect. To increase tumor accumulation, GFMs can be functionalized with targeting ligands. For instance, rGO was modified with PEG and folic acid (FA) (PEG-rGO-FA). Through the synergistic effects of PTT, together with the epacadostat-induced inhibition of indoleamine-2,3-dioxygenase (IDO) and the programmed cell death-ligand 1 (PD-L1) blockade by anti-PD-L1 antibody, PEG-rGO-FA conjugate could effectively eliminate the irradiated tumor and inhibit the growth of a second distant untreated tumor (Figure 1).[37]

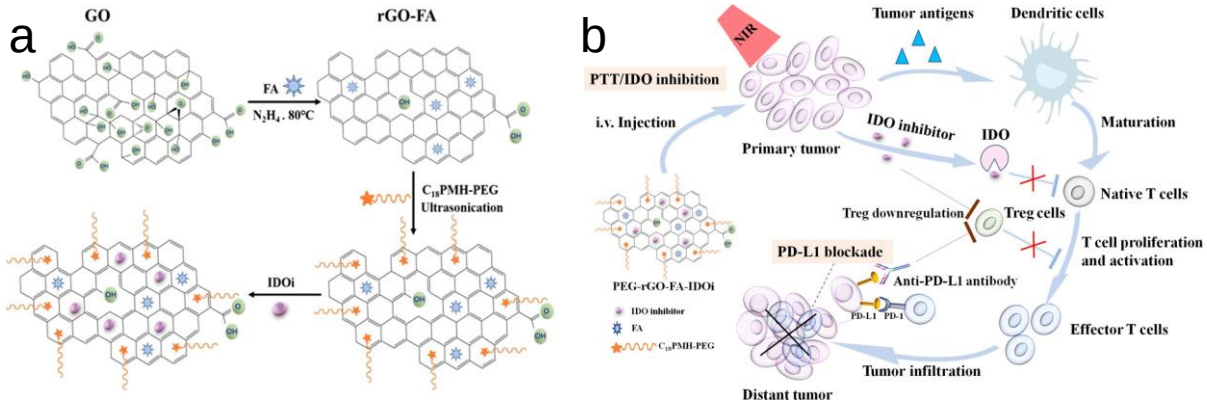

Figure 1. a) Schematic illustration of synthesis of PEG-rGO-FA-IDOi NSs (IDOi, IDO inhibitor). b) PEG-rGO-FA-IDOi mediated PTT/immune (IDO inhibition/PD-L1 blockade) combined therapy for efficient elimination of primary and distant tumors. Reproduced with permission from ref.[37] Copyright 2019, American Chemical Society.

Alternatively, GQDs can be engineered for cancer photo-immunotherapy. In this regard, a multifaceted system made of polydopamine-stabilized GQD/Ce6 nanocomplexes, immunostimulatory polycationic polymer/CpG ODN nanoparticles, and Gd^{3+}/Cy3 imaging probes was designed for dual magnetic resonance/fluorescence imaging-guided photothermal/photodynamic/immune combined therapy.[38] Another alternative system consisting on PEG-GQDs was demonstrated to generate high ROS levels under laser irradiation. In addition, antitumor immune-related cytotoxic T lymphocytes (CTLs) and pro-inflammatory cytokines (e.g., IFN-γ and TNF-α) could be significantly increased after laser irradiation, without the assistance of specific immune regulators, following a strong tumor ablation in the case of oral squamous cell carcinoma.[39] These examples illustrate how photoimmune-combined cancer therapy based on

graphene materials is widening its potential in nanomedicine.

Beside these promising applications, it is worth noting that some GFMs can cause themselves an immune response. After internalization, GO was found to induce a high production of pro-inflammatory cytokines and chemokines (such as IL-6, IFN-γ, TNF-α and MCP-1), while no significant changes were measured for the immunosuppressive cytokines (e.g., IL-10). After PEGylation, PEG-GO (GOP) could further promote the production of these cytokines though the interaction between GO and the macrophage membrane. The study evidenced that this conjugate preferentially adsorbed onto the cell membrane and partially inserted into cell membrane triggering mechanotransduction.[40, 41] Importantly, a single injection *in vivo* enhanced the immune response, indicating that a PEGylated GO could be chosen as an ideal adjuvant for immunotherapy. However, several researchers reported that GO could also significantly inhibit pro-inflammatory cytokine production and reduce intracellular ROS.[42, 43] For example, Han *et al.* demonstrated that GO can behave as natural antioxidants, attenuating inflammatory M1 macrophage polarization by reducing intracellular ROS, and further polarizing M1 macrophages into anti-inflammatory M2 phenotypes by delivering interleukin-4 plasmid DNA in the treatment of myocardial infarction.[43] The inconsistency of the effects of GO on immune response can be attributed to the surface oxidation state of GO.[44] Indeed, GO with a high oxidation degree can easily trigger inflammatory response, meaning that this kind of GO is a suitable candidate for immune cancer therapy. To further assess the intrinsic immune response of GFMs, it will be important to guarantee the actual efficiency *in vivo* when applied to immune cancer therapy. Finally, in term safe use of this type of materials *in vivo*, several articles have demonstrated that highly dispersed GO and GQDs can be rapidly biodegraded by endogenous peroxidases.[45-47] In this context, GO and GQDs possess high potential in future clinical applications for cancer therapy and regulation of inflammation, mainly based on the possibility of surface modification capability and good biodegradability. However, the long-term safety *in vivo* still needs more attention, particularly on the investigation of the impact of GO and GQDs accumulation on the different tissues and organs. Furthermore, the stability of the dispersion is also an issue of concern when GO, GQDs and other types of 2D materials are intravenously injected, and it determines the blood circulation time. Indeed, the nanomaterials should have a long circulation period to let them accumulating more and more into the tumor site, thus enhancing the efficiency of the treatment.

2.2. Xenes Materials

2D Xenes are made of mono-elements, which belong mainly to the periodic table group IV and V (e.g., black phosphorus, antimonene, borophene, and bismuthene). Due to their distinctive properties, such as ultrahigh surface area-to-volume ratio, excellent optical/electronic features and sensitive pH-response, Xenes have attracted the attention also in nanomedicine, for cancer diagnosis and therapy, drug delivery and imaging, and are currently considered as the next generation biocompatible materials,[48] and possess great potential in immune-combined cancer therapy.

Black phosphorus (BP) is widely studied due to its high biocompatibility and good biodegradability. Branched PEI-PEG modified BP loaded with CpG (BPCP) via electrostatic attraction could serve as an effective modulator of necroptosis (a programmed form of necrosis) to mediate PTT, and antitumor immunotherapy by triggering the immunogenic cell death effect and initiating immune response (Figure 2a).[49] Through BP mediated PTT, cancer cells showed necrotic morphologies with certain nuclear swelling and structural change of calcium binding protein calreticulin (CRT) (Figure 2b). Meanwhile, the intracellular expression and the extracellular secretion of HMGB1 (high-mobility group box 1) protein increased (Figure 2c and d). In addition, BP mediated PTT could significantly stimulate adenosine triphosphate (ATP) secretion from cancer cells (Figure 2e). These results evidence the necroptosis process of cancer cells induced by BP-mediated PTT. *In vivo* results have confirmed that this therapeutic modality could activate immune responses and alleviate immunosuppressive tumor microenvironment by the action of T lymphocytes and various cytokines. Indeed, after NIR laser irradiation, the temperature of tumor tissues in BPCP and BP groups rapidly increased to ~45.6 °C, leading to necroptosis (Figure 2f and g). The combined treatment of CpG and BP-mediated PTT achieved efficient photothermal ablation of large solid tumors and immunomodulation leading to eliminate discrete tumorlets (Figure 2h and i). No evident body weight loss was measured during treatment, meaning a low systemic toxicity. The control treatment only based on CpG or BP-mediated PTT showed instead a low efficacy on both primary and distant tumors. Alternatively, BP-based core-shell composites containing a mutated B-raf inhibitor (e.g. dabrafenib), the immune checkpoint inhibitor PD-L1, and the cancer-targeting antibody CXCR4 were designed for photoimmunotherapy with high efficacy, and exhibited cancer targeting and regulation of PD-L1 expression both *in vitro* and *in vivo*.[50]

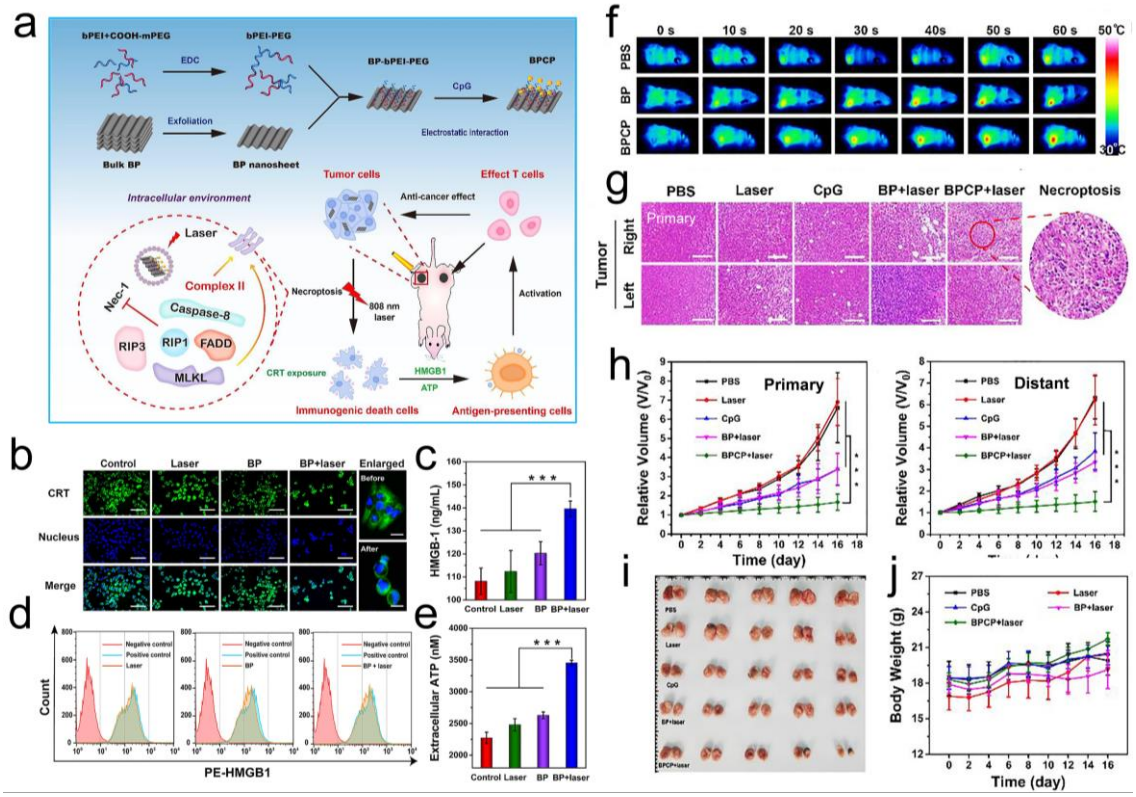

Figure 2. a) Schematic illustration showing the synthetic process to prepare BPCP, the necroptosis

mechanism induced by BP-based PTT, and BPCP-mediated antitumor immune responses for combined cancer therapy. b) Fluorescence staining of CRT. c and d) Measurements of the extracellular secretion and the intracellular expression of HMGB1, respectively. e) Extracellular ATP secretion content after the different treatments. f) Infrared thermal images after exposure to 808 nm laser irradiation. g) H&E staining of the primary and distance tumor tissues after photo-immunotherapy. h) Relative volume change of primary and distance tumors in the different groups. i) Photographs of tumors collected from the different groups after 16-day treatment. j) Body weight change during the treatments. Reproduced with permission from ref. [49].Copyright 2020, Elsevier.

Besides BP, other 2D Xenes have been also exploited in immunotherapy. For instance, palladium nanosheets (Pd NSs) were exploited as carriers of immunoadjuvant CpG ODN and for PTT to enhance their immunotherapeutic effects.[51] Many new Xenes materials, such as borophene,[52] tellurene[53] and bismuthene,[48] just started to be applied in the biomedical field, but not in immune cancer therapy yet.

After entering the physiological environment, nanomaterials are immediately surrounded by a complex and tightly bound protein corona layer, which forms the interface with cells and controls the nanomaterial fate *in vivo*.[54, 55] For example, it has been reported that the protein corona exerts a clear effect on the interaction between BP and immune cells. After the adsorption of plasma proteins (mainly immune relevant proteins) onto BP, the BP-corona complexes showed a pro-inflammatory effect and enhanced ROS production, beneficial to induce cancer cell death.[56] The BP-corona complexes could also interact with calmodulin (an ubiquitously expressed Ca^{2+} binding protein) to activate stromal interaction molecule 2 and facilitate Ca^{2+} influx in macrophages, promoting the polarization of M0 macrophages into M1 phenotype by inducing the activation of p38 and NF-κB pathways.[57] This immune perturbation could promote cancer therapy. Similarly, bare borophene NSs did not provoke immune responses mediated by macrophages, while the protein corona endowed this material with pro-inflammatory and immunoregulatory activity.[58] Interestingly, BP NSs showed a strong immunoregulation either in the presence or not of protein corona. This behavior indicates that the immune response of different 2D Xenes has different degrees of dependence on protein corona. For instance, by proteomics analysis, 46.5% of the proteins in the corona surrounding borophene NSs was composed of immune relevant proteins. This percentage increased to 75.6% in the corona around BP NSs, endowing BP NS-corona complexes with the stronger proinflammatory effect. Overall protein corona seems to have significant effects in tuning the immune responses of 2D Xenes, and corona modification can be used as a promising strategy to improve immune response to further promote cancer therapy. Besides, BP can be easily oxidized by H_2O_2 and gradually degraded by O_2 dissolved in water.[59] These conditions are easy encountered *in vivo*. Therefore, BP can be considered as an ideal candidate in future clinical applications for cancer therapy and inflammation regulation due to its good biodegradability and safety. However, how to efficiently avoid the oxidization of BP during preparation and therapy and how to store BP conjugates for long term before use still need a lot of

attention and efforts.

2.3. MXenes Materials

Since their discovery in 2011, MXenes have attracted a lot of attention as new types of 2D materials.[60] The typical formula of MXenes is $M_{n+1}X_n$, where M is an early d-transition metal, and X is a carbon and/or a nitrogen. The applications of MXenes in combined immune cancer therapy are flourishing. However, only two typical MXenes have been exploited until now. A drug delivery system made of titanium carbide was designed for photothermal/photodynamic/chemo/immune combined cancer therapy (Figure 3a). Ti_3C_2@Met@CP NSs were obtained by layer-by-layer adsorption of metformin [Met, a mechanistic target of rapamycin (mTOR) signalling pathway inhibitor] and compound polysaccharide (CP) (a mixture of lentinan, pachymaran, and tremella polysaccharides) on the surface of Ti_3C_2 NSs (Figure 3b).[61] After hydrogen fluoride delamination and tetramethylammonium hydroxide (TMAOH) intercalation, Ti_3C_2 NSs results in an ultrathin single-layer and highly crystalline microstructure (Figure 3c). This complex possessed several advantages, including a high photothermal conversion efficiency, an effective singlet oxygen generation, a high drug loading capacity (up to 96.2%), a pH-responsive and NIR laser triggered on-demand drug release, an enhanced biocompatibility, and an immune activation. After NIR laser irradiation, the temperature increased in tumor site to 46.3 °C, leading to an efficient photothermal effect and to an on-demand drug release (Figure 3d). Further, CP onto Ti_3C_2 NSs augmented the use proportion of Ti_3C_2@Met@CP at the tumor site (Figure 3e and f). This combined therapy had almost no effect on body weight during the treatment period, indicating little adverse effects on the general health of the mice (Figure 3g). Through the combination of PTT/PDT/chemotherapy/immunotherapy, Ti_3C_2@Met@CP nanocomposite could guarantee a complete tumor eradication and an effective inhibition of tumor recurrence and metastasis (Figure 3h and i). Furthermore, the main organs of the mice after Ti_3C_2@Met@CP treatment (5 days) showed no significant pathological toxicity, adverse effects or histological changes. By measuring Ti content in urine and feces, we could deduce that this nanocomposite system can be easily excreted from the body. Therefore, Ti_3C_2@Met@CP is highly biocompatible and safe to ensure future clinical applications. However, the long-term biosecurity *in vivo* has still to be carefully assessed.

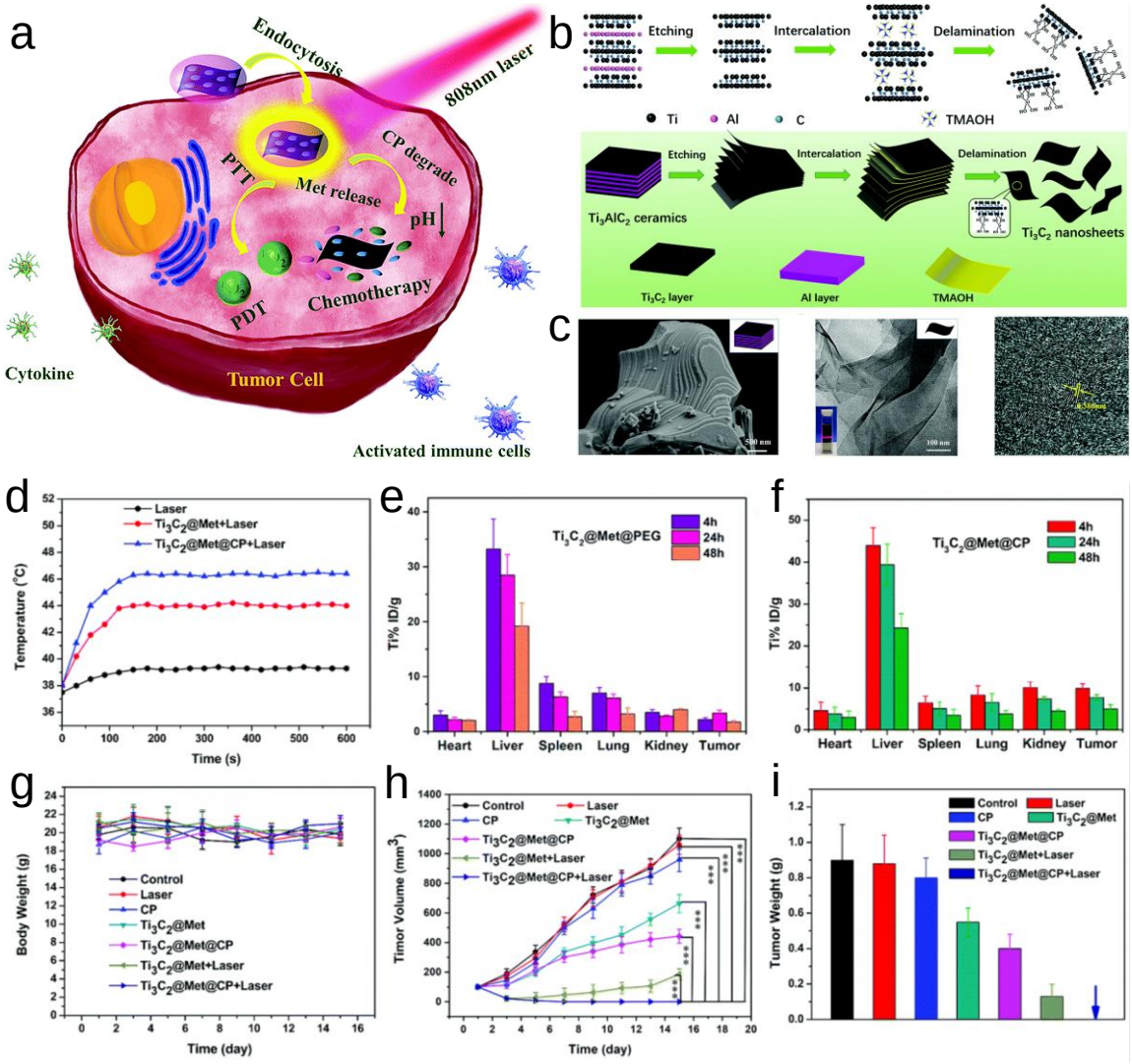

Figure 3. a) Schematic illustration of photothermal/photodynamic/chemo/immune combined therapy mediated by Ti_3C_2@Met@CP NSs. b) Synthetic process of Ti_3C_2@Met@CP NSs by a two-step exfoliation method. c) SEM image of the Ti_3AlC_2 ceramics, and TEM/HRTEM images of the ultrathin Ti_3C_2 NSs after two-step exfoliation. d) Temperature changes of the tumors after the different treatments. e and f) Utilization proportion of Ti_3C_2@Met at the tumor site after PEG and CP modification. g) Body weight change during treatment. h) Tumor volume change during the treatments. i) Tumor weight change after the treatments. Reproduced with permission from ref. [61] Copyright 2020, Royal Society of Chemistry.

Another interesting Mxene is niobium carbide (Nb_2C). A Nb_2C biodegradable bioglass scaffold loaded with the adjuvant imiquimod (IMD) was developed to treat bone metastasis derived from breast cancer.[62] The biodegradability of Nb_2C accounts for a good degree of biosecurity for future applications. *In vivo* results have demonstrated that this engineered scaffold could eradicate primary tumors, activate the immune response, suppress metastases, and prevent tumor relapses by combination of PTT and checkpoint blockade immunotherapy. Further, this scaffold also enhanced the bone regeneration process thanks to the Nb and Si-based degradation products. It is worth noting that the effects of Nb-based degradation products on other organs and tissues

should be analyzed carefully to ensure safely future clinical developments to treat for example cancer and bone tissue defects.

2.4. Transition Metal Dichalcogenides

Transition metal dichalcogenides (TMDs) are widely explored in biomedicine.[63] The most popular TMD is MoS_2 that displays a fast biodegradability in phosphate buffers, being oxidized into water-soluble molybdenum oxide ions, which are rapidly eliminated, thus guaranteeing a high safety use *in vivo* and promising future clinical applications.[64] In this context, a MoS_2-PEG-CpG nanocomposite with a small and uniform size was prepared and used for photothermally enhanced immunotherapy.[65] After modification with CpG and PEG, MoS_2 resulted an efficient adjuvant carrier promoting CpG intracellular accumulation, which could be further improved by photothermal effect. The enhanced uptake stimulated a high production of pro-inflammatory cytokines leading to an efficient immune response. Through PTT and photothermally enhanced immunotherapy, MoS_2-PEG-CpG showed a satisfactory elimination of cancer cells. To further enhance the efficiency of the therapy, MoS_2-based heterostructures can be developed. By the synergetic effects of PTT/CDT/immunotherapy, MoS_2-CuO complexes with multimodal imaging capacity could enhance antitumor efficacy.[66] In this case, CuO provided Cu^{2+} ions for the Haber-Weiss and Fenton-like reactions. Similarly, tumor microenvironment responsive and targeted FePt/MoS_2-FA NSs loaded with CpG ODN (FPMF@CpG ODN) showed a high therapeutic efficiency based on a synergistic PTT/CDT/immunotherapy, and possessed a strong long-term immune memory function to protect the treated mice against tumor recurrence (Figure 4a).[67] FePt nanoparticles anchored onto the surface of MoS_2 catalyzed the Fenton reaction to produce ROS. After 808 nm NIR laser irradiation, FPMF NSs showed the best photothermal performance *in vivo* due to the higher photothermal conversion efficiency, which was sufficient to ablate tumors and limit their proliferation (Figure 4b). With the assistance of an anti-CTLA4 antibody, both primary and distant tumors could be efficiently eliminated by the combination of PTT and immunotherapy (Figure 4c and d). In addition, according to the results of the H&E staining, the major organs presented typical structural phenotypes and did not exhibit histopathological abnormalities or lesions after the different treatments, confirming the high safety and future clinical potential of FPMF@CpG ODN. Similar to BP, attention should be put in the development of protocols to avoid undesired oxidization during therapy and to preserve the functional conjugates (e.g. MoS_2 composites) during long term storage.

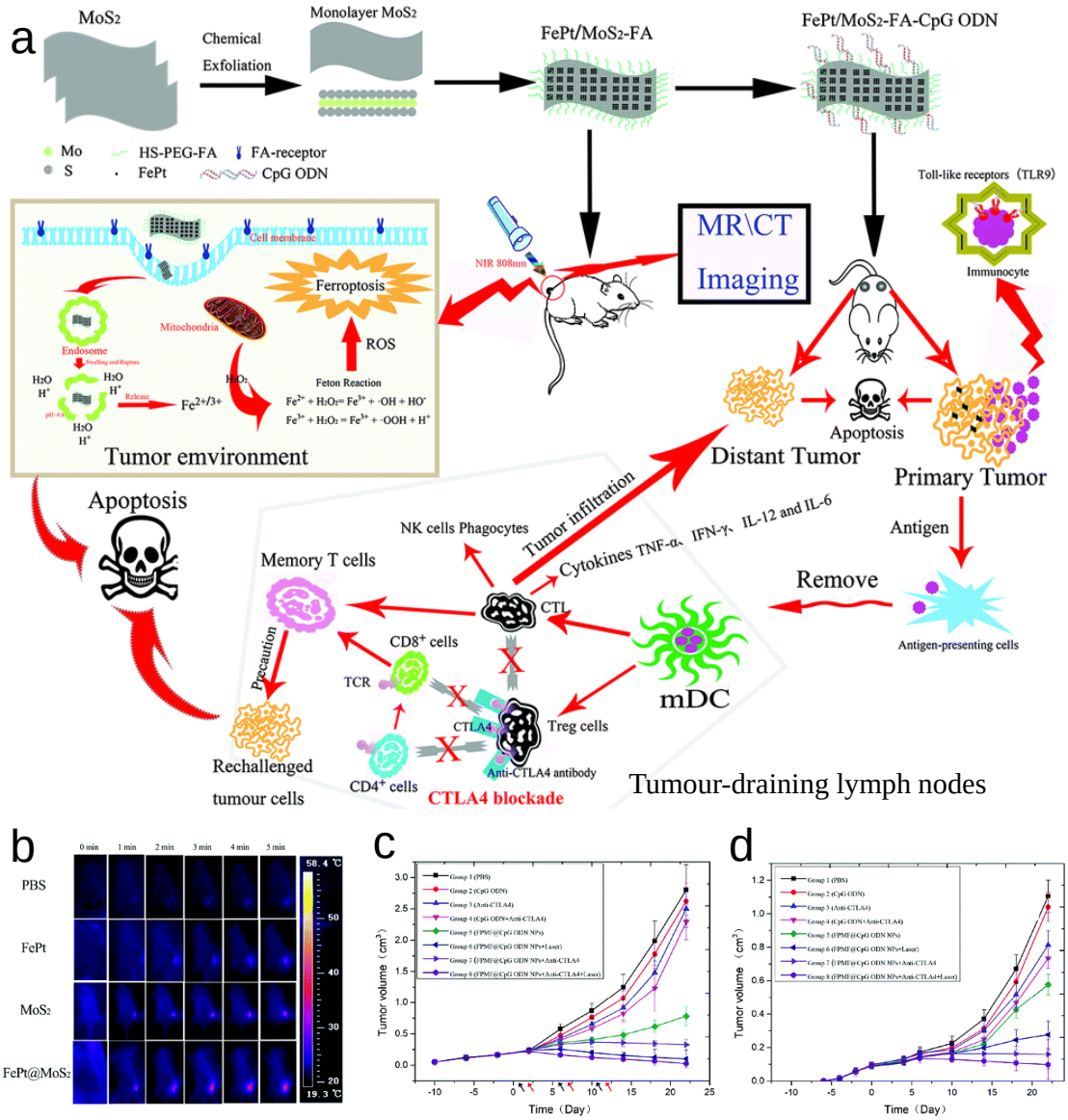

Figure 4. a) Preparation process of FPMF@CpG ODN by chemical exfoliation method and mechanism of FPMF@CpG ODN mediated synergistic PTT/CDT/immunotherapy to eliminate primary and distant tumors. b) Infrared thermal images of 4T1 tumor-bearing mice after intratumoral injection of FePt/MoS_2 NSs under laser irradiation. c and d) Growth curves of primary tumors and distant tumors of bilateral 4T1 tumor-bearing mice after the different treatments. Reproduced with permission from ref. [67] Copyright 2019, Royal Society of Chemistry.

Besides MoS_2, other TMDs also showed great potential in immune cancer therapy. For instance, $MoSe_2$ layers with a high photothermal conversion efficiency were prepared through liquid exfoliation.[68] After coating with red blood cell (RBC) membranes, this material resulted highly hemocompatible and remained in circulation for long time, preventing phagocytosis by macrophages (Figure 5a, left). By combination with anti-PD-1 checkpoint-blockade therapy, the therapeutic efficiency was further improved by blocking the activation of PD-1/PD-L1 pathway (Figure 5a, right). This allowed to avoid the immune failure of CTLs, stopping the transmission of an antiapoptotic signal to tumor cells. After the treatment with RBC-$MoSe_2$ NSs and 808 nm NIR

laser irradiation, the primary tumors almost disappeared, and the distant tumors scarcely grew due to the checkpoint-blockade of anti-PD-1 (Figure 5b). Meanwhile, the survival rate of mice remained 100% within 21 days (Figure 5c). To confirm that the highly synergistic antitumor effects were related to the activation of immunological responses by RBC-$MoSe_2$, the percentage of CTLs (mainly CD3+CD8+ T cells) was analyzed by flow cytometry. It was obvious that PTT enhanced the activation and infiltration of CD3+CD8+ T cells in the tumor tissue (Figure 5d). Moreover, hematological analysis and H&E staining of the main organs demonstrated that RBC-$MoSe_2$ can be considered safe. Therefore, the combination of RBC-$MoSe_2$ with anti-PD-1 checkpoint blockade therapy provides promising advances in personalized PTT-triggered immunotherapy towards clinical translation to treat cancer. In another example, a $WO_{2.9}$-WSe_2-PEG hybrid was designed to obtain a synergistic RT/PTT/checkpoint blockade immunotherapy (anti-PD-L1) for enhanced antitumor and antimetastatic effect.[69] $WO_{2.9}$ NPs were first generated via a hydrothermal treatment, and $WO_{2.9}$-WSe_2 heterostructures were then obtained by selenizing $WO_{2.9}$ NPs. It is worth noting that, through a radiosensitizing mechanism that effectively produced hydroxyl radicals (HO•) and PTT, RT could display a high efficiency under low radiation dose and thus decreased the side effects.

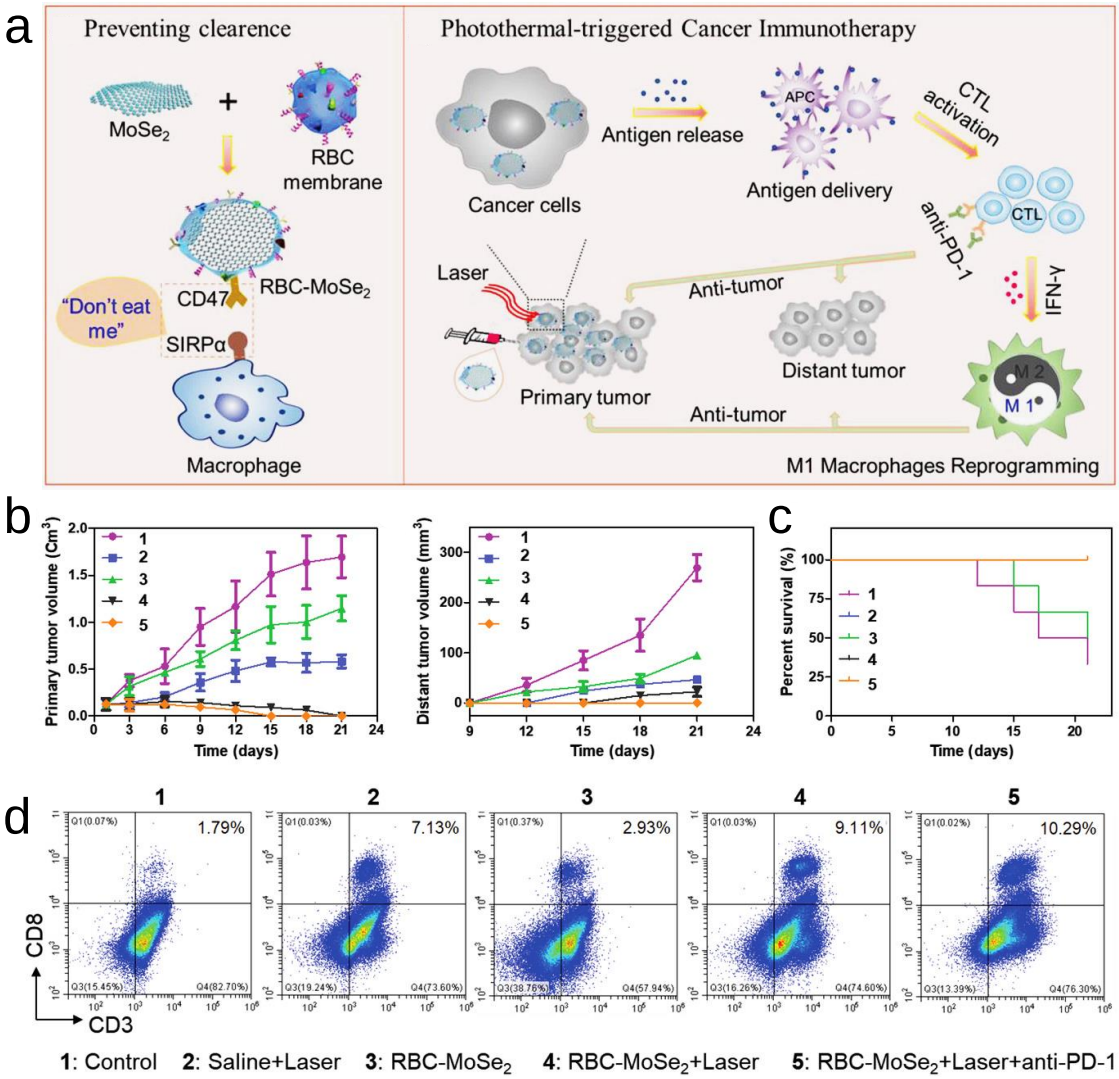

Figure 5. a) Rational design and synthesis of RBC membrane–coated $MoSe_2$ NSs to prevent

macrophage phagocytosis during circulation and schematic illustration of RBC-$MoSe_2$ NSs for efficient photothermal-triggered cancer immunotherapy. b) Volume change of primary and distant tumors after the different treatments. c) Survival percentage of BALB/c mice. d) Percentage of infiltrated CD8+ T cells in primary tumor analyzed by flow cytometry. Reproduced with permission from ref. [68] Copyright 2019, Wiley-VCH.

In a different study, MoS_2 NSs could intrinsically enhance DCs maturation, migration and T cell proliferation.[70] Interestingly, *in vitro* results demonstrated that different immunological responses happened when different blood protein corona (made of human serum albumin/HSA, transferrin/Tf, fibrinogen/Fg, or immunoglobulin G/IgG) were formed around MoS_2 NSs.[71] After adsorption, the protein corona could reduce the surface charges of MoS_2 NSs accompanied by changes in secondary structures of the proteins. Although all MoS_2 NS-protein complexes could trigger an inflammation process, it was evidenced that IgG-coated MoS_2 NSs showed the highest cellular uptake and caused the strongest inflammatory response. Similarly, Fg-coated MoS_2 NSs could also efficiently stimulate the immune response. MoS_2 NSs adsorbed a large amount of IgG but caused a minor change in the β-sheet structure of the antibody, likely due to the structural similarities between MoS_2 NSs and β-sheets in IgG. The loaded IgG was beneficial for the binding to the macrophage receptors (Fc gamma receptors, FcγRs), subsequently promoting the uptake of MoS_2 NSs, inducing macrophages to produce more inflammatory cytokines than the other three MoS_2 NSs-protein complexes. Therefore, the immune-related proteins (such as IgG and Fg) can be used as a coating on 2D materials to increase cellular uptake by macrophages and consequently trigger a higher production and release of cytokines. Furthermore, the molecular mechanism of macrophage-based immune responses induced by PEGylated MoS_2 was analyzed.[72] Due to the enhanced membrane penetration, MoS_2-PEG triggered a longer stimulation and higher cytokine secretion in macrophages than pristine MoS_2.

Similar to GO, the surface conjugation of TMDs can influence the immune responses. Protein corona components, chemical modifications and oxidation degree have obvious effects on the immune response, which gives a clue to design more efficient TMDs for immune cancer therapy. However, not all TMDs are suitable for immune cancer therapy. Indeed, niobium diselenide was demonstrated to effectively eliminate reactive oxygen and nitrogen species via hydrogen atom transfer and redox reaction, following inhibition of inflammation, likely reducing the efficacy of cancer treatment.[73]

2.5. Transition Metal Oxides

Another class of 2D materials explored in the biomedical field is transition metal oxides (TMOs). In particular, they are applied in cancer therapy because they are able to oxidize intracellular reducing substances and promote Fenton reactions by converting H_2O_2 into $HO^{\bullet}$. MnO_2 is among the most commonly used 2D TMOs, with great potential in immune cancer therapy. For example, PLGA-Ce6-MnO_2 coated with 4T1 cancer cell membrane fragments (PCM@M) was designed as

a biomimetic nanoplatform for enhanced PDT and immune activation.[74] PCM@M showed an efficient homologous targeting of 4T1 tumor. Under laser irradiation, PCM@M alleviated tumor hypoxia, promoted macrophage M1 polarization in the tumor microenvironment (TME), and also activated T cells and maturated DCs *in vivo*. To enhance the stability of CDT, another TME-responsive and biodegradable MnO_2/$CaCO_3$ nanoplatform loaded with indocyanine green (ICG) and PD-L1 siRNA was prepared to achieve an enhanced photodynamic/immune combined cancer therapy.[75] $CaCO_3$ layer could enhance ICG stability due to the formation of aggregates, following stronger and longer photodynamic reaction.

In another approach, bimetallic oxide $FeWO_X$-PEG NSs were designed as multifunctional cascade reactors (Figure 6a).[76] $FeWO_X$-PEG NSs showed an efficient catalytic reactivity to convert H_2O_2 into $HO^{\bullet}$ for CDT following the redox reactions that involve Fe^{2+}/Fe^{3+} and W^{5+}/W^{6+} (Figure 6b). The high-valence metal ions Fe^{3+}/W^{6+} are reduced to Fe^{2+}/W^{5+} by glutathione (GSH), respectively, both depleting intracellular GSH (Figure 6c), and amplifying further the oxidative stress, which significantly improved the RT efficacy. Meanwhile, ROS-induced inflammation could activate the immune system to promote tumor infiltration with various types of immune cells. Compared to single $FeWO_X$-PEG or anti-CTLA-4 treatment, $FeWO_X$-PEG plus anti-CTLA-4 modalities showed a remarkable inhibition of primary and distant tumors (Figure 6d and e). As expected, the survival time of mice that underwent $FeWO_X$-PEG plus anti-CTLA-4 combination was prolonged (Figure 6f). According to the flow cytometry analysis results, the largest percentage of DC maturation and the consequent decrease of T_{reg} cells were found in $FeWO_X$-PEG/anti-CTLA-4 group, which confirmed that the immune response played a significant role in the efficient cancer therapy (Figure 6g). Interestingly, this type of 2D materials (e.g., MnO_2 and $FeWO_x$) are pH responsive, meaning that they can be easily degraded in acid condition and then expelled from body. This acid responsive degradation behaviour renders 2D TMOs highly safe for future clinical translation. However, one disadvantage is that they can be reduced by reducing substances such as GSH, cysteine or ascorbic acid that are present in our body. Therefore, maintaining the chemical stability of 2D TMOs during blood circulation is fundamental to achieve high therapeutic efficacy and promote the future clinical applications. For this purpose, one possible strategy might be to prepare specific material coating to inhibit redox reactions during blood circulation.

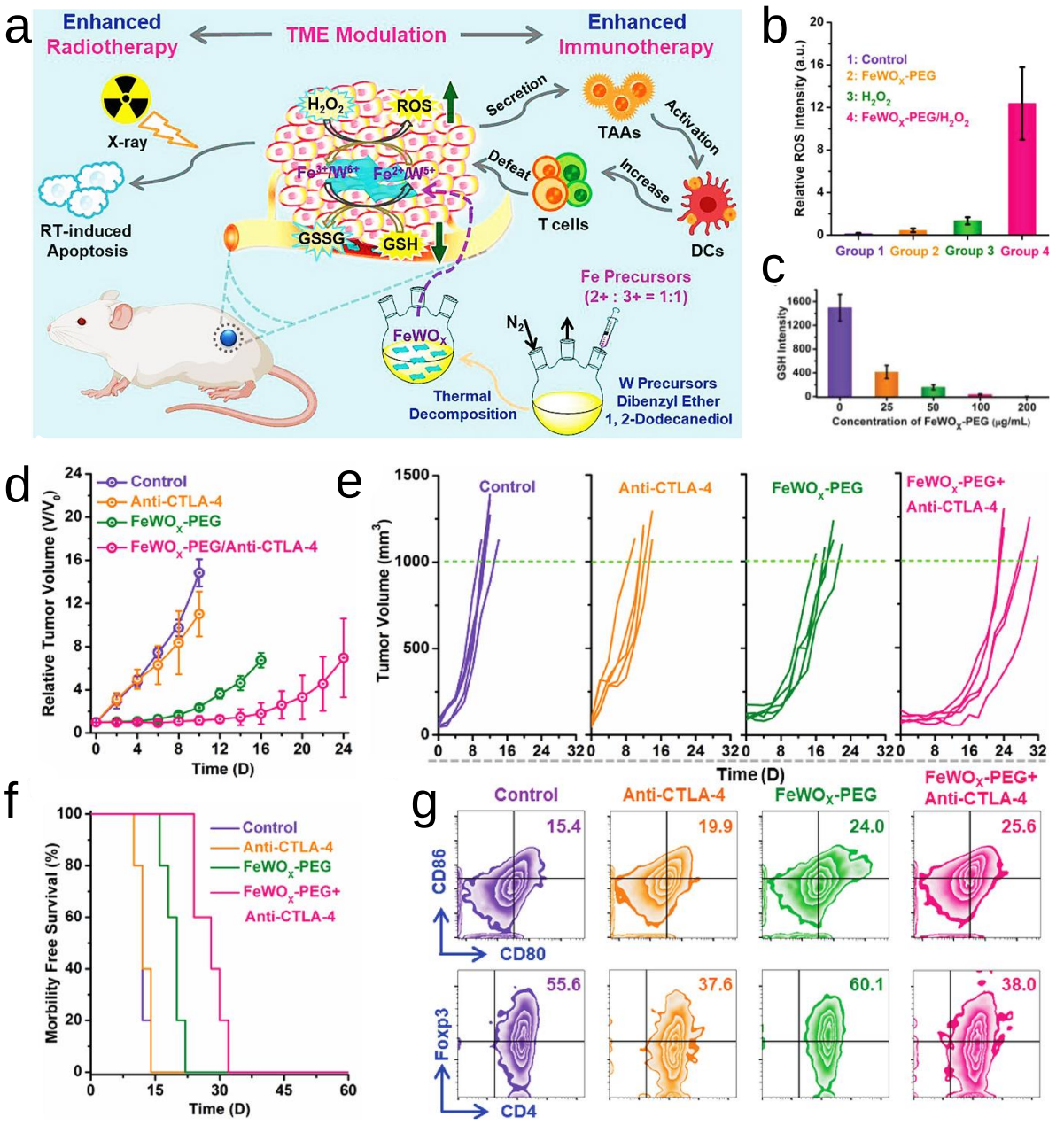

Figure 6. a) Schematic illustration of $FeWO_X$-PEG NSs with efficient TME-modulation performance for enhanced RT and immunotherapy. b) ROS content after different treatment. c) GSH depletion after treatment with $FeWO_X$-PEG. d and e) Relative tumor volume and tumor volume change. f) Survival curves of mice following the different treatments. g) Representative flow cytometric analysis of DC maturation (CD80+CD86+) within the lymph and T_{reg} cells (CD4+Foxp3+) inside the tumor. Reproduced with permission from ref. [76] Copyright 2020, Wiley-VCH.

2.6. Metal-Organic Frameworks

Metal-organic frameworks (MOFs), an emerging class of nanocarriers, have become powerful tools for cancer immunotherapeutics with improved stability, efficacy and safety.[77, 78] MOFs can be also engineered in bidimensional structures. Cationic W-TBP NSs (composed of W^{6+} ions and the photosensitizer 5,10,15,20-tetra(*p*-benzoato)porphyrin, TBP) could mediate PDT to release

tumor-associated antigens and deliver CpG, loaded onto the sheets, to DCs. The synergy of the enhanced antigen presentation and checkpoint blockade (α-PD-L1) immunotherapy expanded and reactivated cytotoxic T cells, achieving satisfactory anticancer efficacy and robust abscopal effects with >97 % tumor regression combined with W-TBP NSs-mediated PDT.[79] In contrast, while W-TBP/CpG showed a strong local tumor control, it had almost no effect on distant tumors under light irradiation. It is worth noting that α-PD-L1 immunotherapy can only supress primary tumors slightly, and was ineffective against the distant tumors. To further improve the therapeutic efficiency, W^{6+} ions were replaced by Cu^{2+} ions, which could exert excellent CDT.[80, 81] Due to the biodegradability, Cu-TBP NSs efficiently released Cu^{2+} and TBP intratumorally. Copper ions catalyzed E2 metabolism to generate different types of ROS, while TBP irradiated at 650 nm triggered PDT, which suppressed the tumor growth. Combined to α-PD-L1 immunotherapy, the system could eradicate local tumors and regressed distant tumors through systemic antitumor immunity.

It has been demonstrated that MOF NSs made of heavy-metal secondary building units and photosensitizing ligands could mediate efficiently RT/RDT by enhancing X-ray energy deposition and generating multiple ROS.[82] For example, Hf-anthracene MOF was able to absorb X-ray photons leading to RT (via the production of $HO^{\bullet}$) and perform RDT (by exciting the photosensitizers to generate $^1O_2$). Based on this, Hf-DBP (5,15-di(p-benzoato)porphyrin) and Hf-DBP-Fe nanoplates were used for immune combined cancer therapy. Hf-DBP was loaded with IDOi enabling a synergistic RT/RDT and immunotherapy under very low doses of X-rays.[83] Importantly, the combination of IDOi and antigen release from local X-ray-induced immunogenic cell death triggered the effective expansion and tumor infiltration of $CD8^+$ T cells, leading to the eradication of the untreated tumors. This system could be further engineered by loading IMD and anti-CD47 antibody on the Hf-DBP nanoplates (IMD@Hf-DBP/αCD47) to repolarize immunosuppressive M2 macrophages into immunostimulatory M1 macrophages and block CD47 tumor cell surface marker to promote phagocytosis (Figure 7).[84] Under X-ray irradiation, IMD@Hf-DBP/αCD47 could regulate the immunosuppressive microenvironment and activate innate immunity to orchestrate adaptive immunity when synergized with α-PD-L1, leading to complete eradication of both primary and distant tumors. Moreover, to overcome hypoxia and perform CDT, the Hf-DBP nanoplates can be modified with iron.[85] Endowed with a catalase-like activity, Hf-DBP-Fe could decompose H_2O_2 into hypoxic tumors to generate O_2 and $HO^{\bullet}$. The generated O_2 enhanced radiodynamic therapy. Through the synergistic combination with anti-PD-L1, Hf-DBP-Fe eradicated primary tumors and distant tumors through systemic antitumor immunity. Although the safety aspects of 2D MOF described above have been demonstrated by the results during cancer therapy (no changes on body weight and organ pathology), the long-term impact needs further assessment. In addition, the biodegradability *in vivo* and excretion from body of 2D MOFs has also to be investigated before clinical translation.

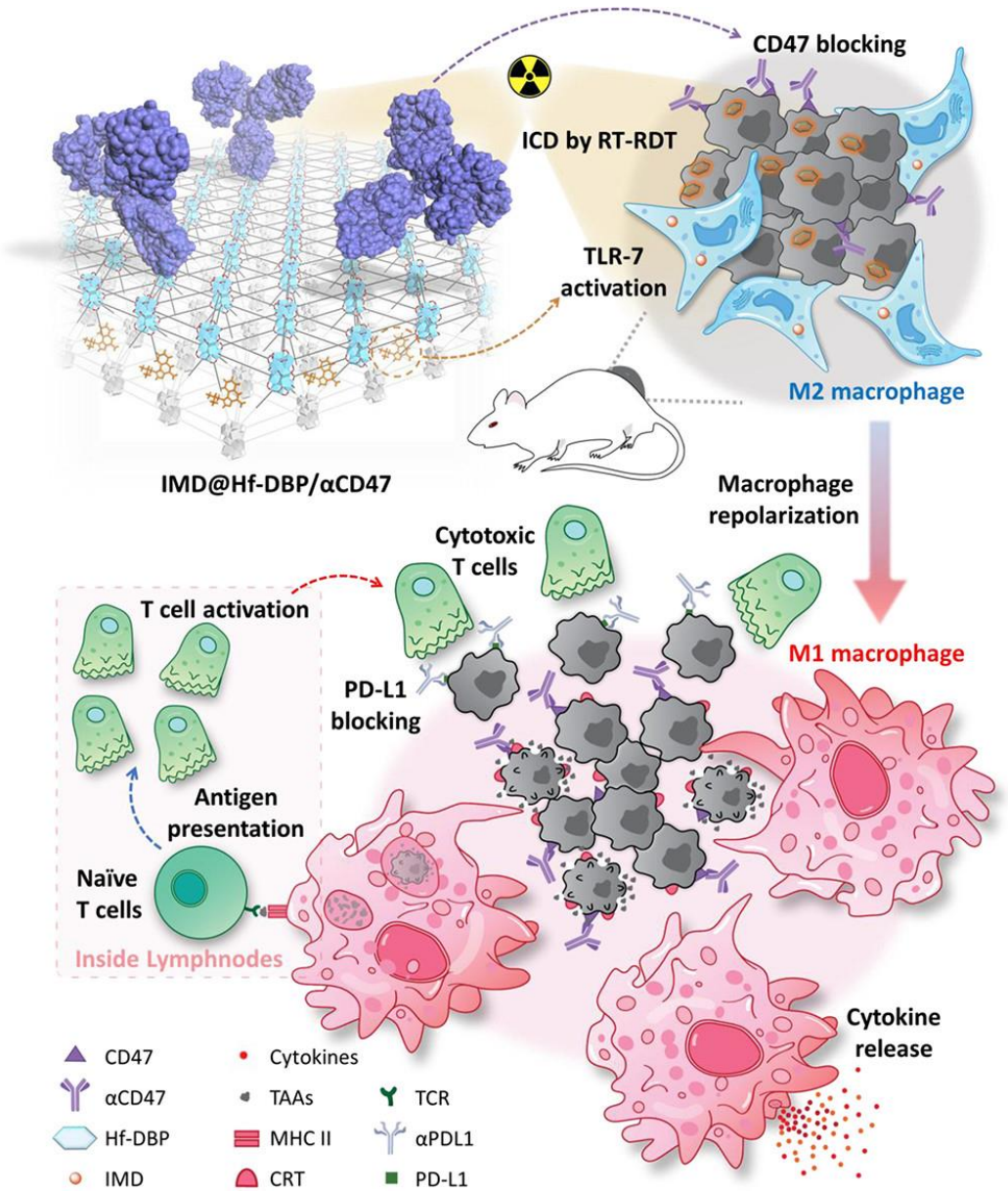

Figure 7. Schematic mechanism of IMD@Hf-DBP/αCD47 nanoplates-based RT and RDT activity, modulating the immunosuppressive tumor microenvironment (M2 to M1 repolarization of macrophages) and activating innate immunity when synergized with an anti-PD-L1. Reproduced with permission from ref. [84] Copyright 2020, American Chemical Society.

2.7. Layered Double Hydroxides

Layered double hydroxides (LDHs) are a type of anionic clay with the general chemical formula $[M^{2+}_{1-x}M^{3+}_{x}(OH)_2]\ [A^{n-}]_{x/n}\bullet zH_2O$ (where M^{2+} is the bivalent metal cations, M^{3+} is the trivalent metal cations, A^{n-} is the interlayer anions, and x usually varies from 0.2 to 0.4).[86] LDHs possess two typical advantages in nanomedicine: (a) hydroxyl groups sensitive to an acid environment leading to the release of therapeutic molecules in a pH-responsive way, and (b) positive charges allowing the material to effectively interact with negatively charged cell membranes for efficient intracellular delivery.[87, 88] For example, MgAl-LDHs were able to co-deliver ovalbumin and CpG to obtain a high antitumor efficacy by Th1 polarized immune responses.[89] To further improve the therapeutic

action, MgAl-LDHs co-loaded with IDOi and Pt(IV) prodrugs (e.g., disuccinatocisplatin) was designed.[90] Pt(IV)-IDOi/LDHs showed improved cellular accumulation and increased binding of Pt to DNA causing elevated apoptosis. IDOi could reverse immunosuppressive T cells to recognize cancer cells, leading to T cell proliferation and activation, cancer cell cycle arrest, ultimately increasing cancer cell death and suppressing the growth of human cervical tumor. Similar to TMOs, LDHs are also degraded in acid conditions, guaranteeing a high biocompatibility. Meanwhile, to keep the chemical stability of LDHs (due to the presence of ions with high valence states) during blood circulation needs more attention for clinical applications against undesirable redox reaction before achieving tumor site.

2.8. Other 2D Materials

Other types of 2D materials have been also utilized in immune cancer therapy. Covalent organic frameworks (COFs) loaded with ICG were exfoliated by ultrasound and coated with polydopamine (PDA) to construct ICG@COF-1@PDA NSs with photoimmunotherapy activity (Figure 8a).[91] Compared with ICG, ICG@COF-1@PDA NSs had a prolonged circulation time and optimized tumor accumulation (Figure 8b and c), causing higher photothermal effect in tumor (Figure 8d). The impact of ICG@COF-1@PDA-mediated phototherapy on damage-associated molecular patterns (DAMPs) in CT26 tumors was analyzed. Both HSP70 and HMGB1 were obviously upregulated after ICG@COF-1@PDA NSs treatment under NIR laser irradiation (Figure 8e). Meanwhile, ICG@COF-1@PDA&NIR treatment can promote DCs maturation (CD11c+/CD80+/CD86+, Figure 8f). Through PTT and PDT, immunogenic cell death and antitumor immunity were induced in colorectal cancer. Therefore, both primary and distant cancers can be inhibited efficiently, whereas free ICG mediated phototherapy had negligible effect on tumor growth (Figure 8g and h). Additionally, the increased CD8+ T cells infiltrated in distant tumors after ICG@COF-1@PDA&NIR treatment (Figure 8i), and the level of IFN-γ also were obviously elevated (Figure 8j). Therefore, ICG@COF-1@PDA-based PTT/PDT dual mode phototherapy could provide abundant DAMPs to initiate a systemic immune response. Further, the dual mode phototherapy also can effectively ablate invasive tumors and inhibit tumor metastasis. Notably, the reversible covalent bonds in COF can maintain the structure in normal conditions but will be broken under acid condition, confirming the biosecurity of COF-based nanosystem *in vivo*.[92] Moreover, white mica sheets were prepared by polyamine intercalation method, and mainly promoted immunostimulatory M1 polarization of RAW 264.7 macrophages, providing the basis for chemo-combined immune cancer therapy.[93]

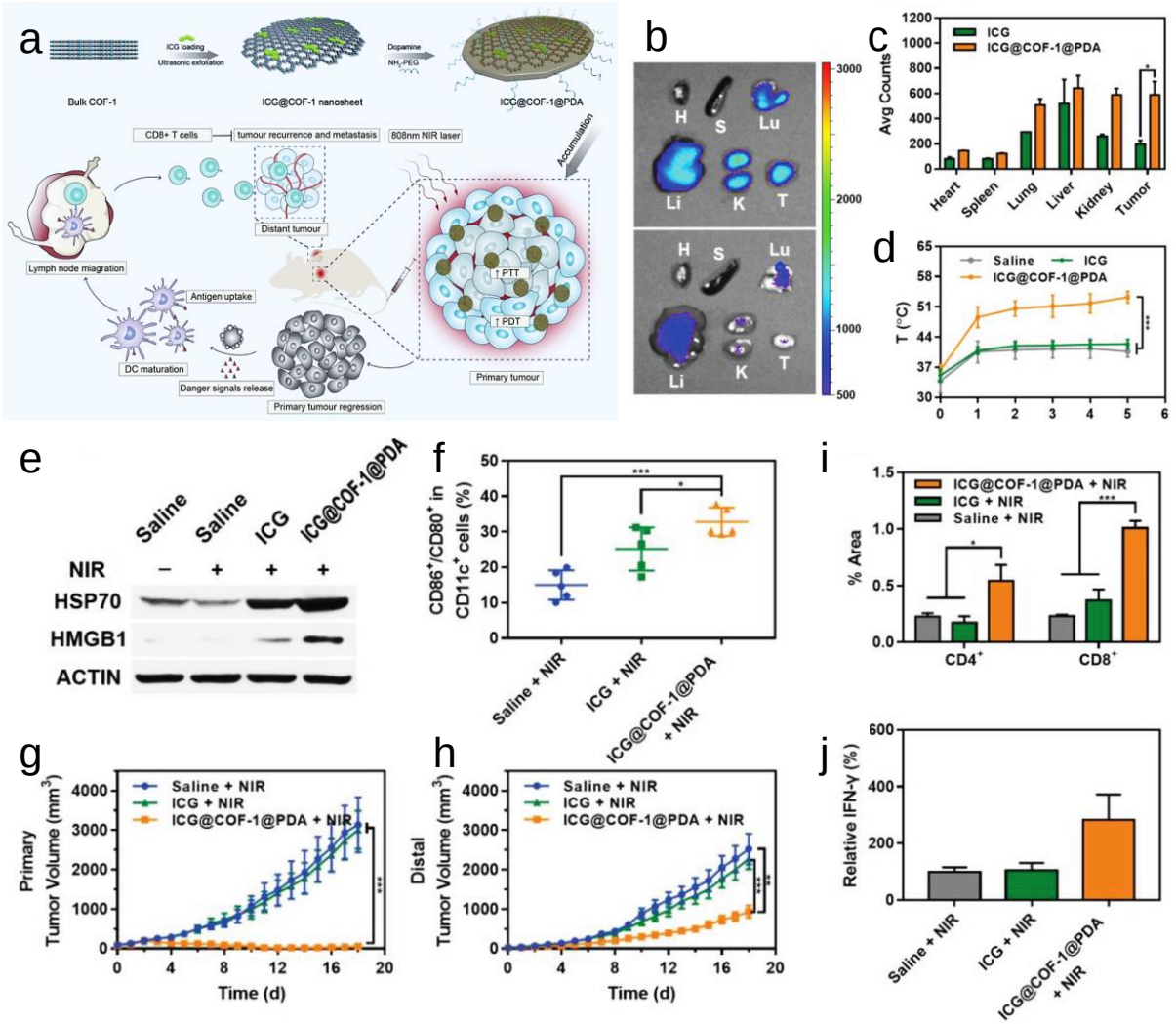

Figure 8. a) Scheme showing the preparation process of ICG@COF-1@PDA NSs and the mechanism of their mediated photoimmunotherapeutic activity. b) *Ex vivo* fluorescence images of major organs and tumors 24 h post i.v. injection. c) Biodistribution of ICG@COF-1@PDA NSs in major organs and tumors at 24 h post-injection. d) Temperature changes recorded by tumor-based on IR thermal imaging. e) HSP70 and HMGB1 expression in tumors after the different treatments. f) Flow cytometry analysis of DC maturation (CD80+/CD86+) in tumor-draining lymph nodes. g and h) Primary and distant tumor volume change during the different treatments. i) Quantitation of mean fluorescence intensities of CD8+ and CD4+ cells. j) IFN-γ levels in distant tumors. Reproduced with permission from ref. [91] Copyright 2019, Wiley-VCH.

3. Summary and Outlook

Taken together, the examples described in this review lead us to conclude that the combination of immunotherapy and other cancer therapies based on 2D materials is extremely effective and safe to eradicate cancer. In immunotherapy applied alone, mild to serious side effects (e.g., nausea, vomiting, lung/skin/gastrointestinal/renal toxicities, hypothyroidism, arthralgia, vasculitis, and autoimmune hepatitis) were evidenced. Actually, besides immunotherapy, other single therapy (such as well-known and clinically approved chemotherapy, PDT, PTT, and RT) also

causes some side effects (e.g., fatigue, hair loss, infection, anemia, nausea and vomiting) and shows relatively low efficiency, and only treats local tumors efficiently rather than distant tumors. Generally, for all types of therapeutic treatments, the way to get better efficiency is to increase the dose, with the risk to trigger more serious side effects. Through the synergistic effects provided by the different therapies, their combination is becoming a popular and satisfactory strategy to overcome these side effects and to enhance the therapy outcome. Therefore, 2D materials mediated immune-combined therapy was put forward as an advanced solution. The combined therapeutic approaches are mainly dictated by the multiple properties of 2D materials. Usually, 2D materials are used as carriers to promote cancer immune therapy due to their large specific surface area and efficient complexation with other molecules. By utilizing other functions of 2D materials, immune cancer therapy could be combined with one or more therapeutic strategies, including chemotherapy, PTT, PDT, CDT, RDT, and RT, leading to higher therapeutic efficiency, minor side effects and good safety. These different combined modes based on different 2D materials have been summarized in **Table 1**.

Table 1. Classification and applications of 2D materials in immuno-combined cancer therapy.

Class of Materials	Type of Materials	Combined Modes	*In vivo* Models	Ref.
GFMs	GO	Immunotherapy/PTT	CT26 colon carcinoma tumor-bearing BALB/c mice	[34]
			Osteosarcoma-bearing BALB/c nude mice	[36]
	rGO	Immunotherapy/PTT	CT26 colon carcinoma tumor-bearing BALB/c mice	[37]
	GQDs	Immunotherapy/PDT/PTT	EMT6 tumor-bearing BALB/c mice	[38]
		Immunotherapy/PDT	SCC VII tumor-bearing C3H mice	[39]
Xenes	BP	Immunotherapy/PTT	4T1 tumor-bearing BALB/c mice	[49]
		Immunotherapy/PTT	B-16 tumor-bearing C57BL/6 mice	[50]
	Pd	Immunotherapy/PTT	B16F10 tumor-bearing C57BL/6 mice	[51]
MXenes	Ti_3C_2	Immunotherapy/chemotherapy /PDT/PTT	MDA-MB-231 tumor-bearing BALB/c nude mice	[61]
	Nb_2C	Immunotherapy/PTT	4T1 tumor-bearing BALB/c mice	[62]
TMDs	MoS_2	Immunotherapy/PTT/CDT	CT26 tumor-bearing BALB/c mice	[66]
		Immunotherapy/PTT/CDT	4T1 tumor-bearing BABL/c mice	[67]
	$MoSe_2$	Immunotherapy/PTT	CT26 colorectal tumor-bearing BABL/c mice	[68]
	$WO_{2.9}$-WSe_2-PEG	immunotherapy/PTT/RT	4T1 tumor-bearing BALB/c mice	[69]
TMOs	MnO_2	Immunotherapy/PDT	4T1 tumor-bearing BABL/c mice	[74]
	$FeWO_X$	Immunotherapy/CDT	4T1 tumor-bearing BABL/c mice	[76]

MOFs	W-TBP	Immunotherapy/PDT	TUBO tumor-bearing BALB/c mice	[79]
	Cu-TBP	Immunotherapy/RT/RDT	B16F10 tumor-bearing C57BL/6 mice	[80]
	Hf-DBP	Immunotherapy/RT/RDT	CT26 tumour-bearing BALB/c mice	[83, 84]
	Hf-DBP-Fe	Immunotherapy/RT/RDT/CDT	MC38 tumor-bearing C57BL/6 mice	[85]
LDHs	MgAl-LDHs	Immunotherapy/chemotherapy	HeLa tumor-bearing BALB/c nude mice	[90]
Other 2D Materials	COF-1	Immunotherapy/PTT/PDT	CT26/4T1 tumor-bearing BALB/c mice	[91]

Although significant breakthroughs have been achieved for immune-combined cancer therapy, some issues and challenges still exist. One of them is that most combined therapeutic modes are lacking of tumor targeting capacity, resulting in high effective doses and potential toxicity. Within the different existing combinations, immunotherapy/PTT is the main exploited mode, while new strategies to integrate more functions (such as PDT and CDT) into one nanosystem are still needed. Meanwhile, the anticancer efficacy is usually assessed in short time, ignoring the risks of cancer recurrence. Furthermore, the effect of the intrinsic properties and of the degradation products on the immune response should be assessed before any therapy. Some solutions will be useful to overcome these challenges. For instance, modification with targeting molecules or coating with cancer cell membranes could endow 2D materials with efficient therapeutic action. The combination of different 2D materials provides an alternative basis for multifunction integration.

We would like to evidence that 2D materials can also regulate themselves the immune responses. During or after cancer therapy, 2D materials or the corresponding degraded products are capable to stimulate the immune system. As we have discussed above, GO with different surface modifications can be immunostimulatory or immunosuppressive, meaning that different types of GO can be used in cancer therapy or in anti-inflammatory processes based on the different immune response. In the case of TMDs, MoS_2 can promote the pro-inflammatory action of macrophages, while $NbSe_2$ oppositely showed an anti-inflammatory function. Besides, white mica sheets were demonstrated to mainly promote immunostimulatory M1 polarization of macrophages, but silicon-containing ions, liberated as product of degradation, were found to induce macrophages to M2 polarization.[94] Therefore, it is essential to carefully choose suitable 2D materials to develop an efficient immune cancer treatment. Interestingly, during tissue repair, sequential M1/M2 phenotype transition is necessary to enhance vascularization and bone remodelling.[95, 96] Therefore, white mica sheets may be an ideal candidate to regulate bone repair. Similarly, BP promoted the polarization of M0 macrophages into M1 phenotype. However, the degradation product phosphate not only induced macrophages to M2 polarization but also promoted osteogenic differentiation and mineralization, which are beneficial for bone repair. Besides, due to the capacity of MnO_2 to convert H_2O_2 into H_2O and O_2, MnO_2 NSs have been used to eliminate inflammation by decreasing ROS level and promote tissue repair by decreasing oxidative stress level.[97]

Furthermore, the formation of protein corona should be also considered, as it affects the immune

responses of 2D materials. Indeed, as for other nanomaterials and nanoparticles, material coronation can regulate the degree of immune responses, and some of plasma proteins can even endow 2D materials, which lack of an intrinsic immune response, with pro-inflammatory and immunoregulatory activity. Importantly, there are still many 2D materials not applied in immune combined cancer therapies, meaning that a lot of work needs to be done to expand the applications to all possible 2D materials. Some of 2D materials (such as GO, BP, MnO_2 and LDHs) are easily degraded while others are inversely more persistent (e.g., rGO and Ti_3C_2). These biodegraded 2D materials usually are pH responsive or easily oxidized, forming water soluble products. A good biodegradability confirms a high biosecurity, and promotes the potential clinical translation.

We would like to evidence that, although some inorganic nanomaterials, including for example nano-Au, nano-iron oxide, and nano-hafnium oxide, are undergoing clinical trials or have been approved by FDA or EMA for chemotherapy, PTT and RT, 2D materials are still missing in this list of trials.[98] The majority of 2D materials are still in preclinical trials, using animal models. Possible reasons that hinder the translation to clinical processes of 2D materials include the complex preparation methods, the still relatively high cost, the low stability, the lack of long-term safety assessment and the low market trust. Gratifyingly, many researchers are paying enormous efforts to promote the clinical translation of 2D materials, accounting for a bright future.

In summary, the synthesis of more intelligent and multifunctional 2D material-based therapeutic systems, with low cost and simple preparation processes, is still challenging. We believe that this review will be useful for better understanding the synergies between immunotherapy and other therapeutic strategies mediated by 2D materials, and could inspire and guide the community of chemists and material scientists on the design of more effective multifunctional 2D materials for the treatment of cancer and other diseases.

Acknowledgements

We gratefully acknowledge the Centre National de la Recherche Scientifique (CNRS), the International Center for Frontier Research in Chemistry (icFRC), and the financial support from the Agence Nationale de la Recherche (ANR) through the Interdisciplinary Thematic Institute ITI-CSC via the IdEx Unistra (ANR-10-IDEX-0002) within the program “Investissement d’Avenir”, and from Qilu Young Scholars Program of Shandong University. The authors are indebted to C. Ménard-Moyon for critically reading this manuscript.

Conflict of interest

The authors declare no conflict of interest.

REFERENCE

[1] H. Zhang, T. Fan, W. Chen, Y. Li, B. Wang, *Bioact. Mater.* **2020**, *5*, 1071–1086.
[2] R. Kurapati, K. Kostarelos, M. Prato, A. Bianco, *Adv. Mater.* **2016**, *28*, 6052–6074.
[3] B. Yang, Y. Chen, J. Shi, *Chem* **2018**, *4*, 1284–1313.
[4] Y. Wang, M. Qiu, M. Won, E. Jung, T. Fan, N. Xie, S.-G. Chi, H. Zhang, J. S. Kim, *Coordin. Chem. Rev.* **2019**, *400*, 213041.
[5] B. Ma, C. Martín, R. Kurapati, A. Bianco, *Chem. Soc. Rev.* **2020**, *49*, 6224–6247.
[6] Y. Chen, L. Wang, J. Shi, *Nano Today* **2016**, *11*, 292–308.
[7] S. Liu, X. Pan, H. Liu, *Angew. Chem. Int. Ed.* **2020**, *132*, 5943–5953.
[8] L. Cheng, X. Wang, F. Gong, T. Liu, Z. Liu, *Adv. Mater.* **2020**, *32*, 1902333.
[9] S. Liu, X. Pan, H. Liu, *Angew. Chem. Int. Ed.* **2020**, *59*, 5890–5900.
[10] T. Hu, X. Mei, Y. Wang, X. Weng, R. Liang, M. Wei, *Sci. Bull.* **2019**, *64*, 1707–1727.
[11] I. Mellman, G. Coukos, G. Dranoff, *Nature* **2011**, *480*, 480–489.
[12] W. Song, S. N. Musetti, L. Huang, *Biomaterials* **2017**, *148*, 16–30.
[13] R. S. Riley, C. H. June, R. Langer, M. J. Mitchell, *Nat. Rev. Drug Discov.* **2019**, *18*, 175–196.
[14] K. M. Hargadon, C. E. Johnson, C. J. Williams, *Int. Immunopharmacol.* **2018**, *62*, 29–39.
[15] K. Ni, G. Lan, C. Chan, B. Quigley, K. Lu, T. Aung, N. Guo, P. La Riviere, R. R. Weichselbaum, W. Lin, *Nat. Commun.* **2018**, *9*, 2351.
[16] J. Fisher, N. Zeitouni, W. Fan, F. H. Samie, *J. Am. Acad. Dermatol.* **2020**, *82*, 1490–1500.
[17] F. Martins, L. Sofiya, G. P. Sykiotis, F. Lamine, M. Maillard, M. Fraga, K. Shabafrouz, C. Ribi, A. Cairoli, Y. Guex-Crosier, *Nat. Rev. Clin. Oncol.* **2019**, *16*, 563–580.
[18] F. Kroschinsky, F. Stölzel, S. von Bonin, G. Beutel, M. Kochanek, M. Kiehl, P. Schellongowski, *Crit. Care* **2017**, *21*, 89.
[19] W. Sang, Z. Zhang, Y. Dai, X. Chen, *Chem. Soc. Rev.* **2019**, *48*, 3771–3810.
[20] J. Nam, S. Son, K. S. Park, W. Zou, L. D. Shea, J. J. Moon, *Nat. Rev. Mater.* **2019**, *4*, 398–414.
[21] Z. Xie, M. Peng, R. Lu, X. Meng, W. Liang, Z. Li, M. Qiu, B. Zhang, G. Nie, N. Xie, *Light-Sci. Appl.* **2020**, *9*, 1–15.
[22] S. Yan, Z. Luo, Z. Li, Y. Wang, J. Tao, C. Gong, X. Liu, *Angew. Chem. Int. Ed.* **2020**, *59*, 17332–17343.
[23] D. Hu, W. Zhang, J. Tang, Z. Zhou, X. Liu, Y. Shen, *Biomaterials* **2021**, *265*, 120407.
[24] J. Liu, R. Zhang, Z. P. Xu, *Small* **2019**, *15*, 1900262.
[25] Q. Liu, Y. Duo, J. Fu, M. Qiu, Z. Sun, D. Adah, J. Kang, Z. Xie, T. Fan, S. Bao, H. Zhang, L.-P. Liu, Y. Cao, *Nano Today* **2021**, *36*, 101023.
[26] Q. Jin, Z. Liu, Q. Chen, *J. Control. Release* **2021**, *329*, 882–893.
[27] D. de Melo-Diogo, R. Lima-Sousa, C. G. Alves, I. J. Correia, *Biomater. Sci.* **2019**, *7*, 3534–3551.
[28] M. A. Lucherelli, Y. Yu, G. Reina, G. Abellán, E. Miyako, A. Bianco, *Angew. Chem. Int. Ed.* **2020**, *59*, 14034–14039.
[29] B. Ma, Y. Nishina, A. Bianco, *Carbon* **2021**, *178*, 783–791.
[30] H. Yue, W. Wei, Z. Gu, D. Ni, N. Luo, Z. Yang, L. Zhao, J. A. Garate, R. Zhou, Z. Su, G. Ma, *Nanoscale* **2015**, *7*, 19949–19957.
[31] X. Wang, F. Cao, M. Yan, Y. Liu, X. Zhu, H. Sun, G. Ma, *Acta Biomater.* **2019**, *83*, 390–399.
[32] C. Xu, H. Hong, Y. Lee, K. S. Park, M. Sun, T. Wang, M. E. Aikins, Y. Xu, J. J. Moon, *ACS Nano* **2020**, *14*, 13268–13278.
[33] C. Loftus, M. Saeed, D. M. Davis, I. E. Dunlop, *Nano Lett.* **2018**, *18*, 3282–3289.
[34] Y. Tao, E. Ju, J. Ren, X. Qu, *Biomaterials* **2014**, *35*, 9963–9971.
[35] M. Klichinsky, M. Ruella, O. Shestova, X. M. Lu, A. Best, M. Zeeman, M. Schmierer, K. Gabrusiewicz, N. R. Anderson, N. E. Petty, K. D. Cummins, F. Shen, X. Shan, K. Veliz, K. Blouch, Y. Yashiro-Ohtani, S. S. Kenderian, M. Y. Kim, R. S. O'Connor, S. R. Wallace, M. S. Kozlowski, D. M. Marchione, M. Shestov, B. A. Garcia, C. H. June, S. Gill, *Nat. Biotechnol.* **2020**, *38*, 947–953.
[36] X. Deng, H. Liang, W. Yang, Z. Shao, *J. Photochem. Photobiol. B* **2020**, *208*, 111913.
[37] M. Yan, Y. Liu, X. Zhu, X. Wang, L. Liu, H. Sun, C. Wang, D. Kong, G. Ma, *ACS Appl. Mater. Interfaces* **2018**, *11*, 1876–1885.
[38] C. Wu, X. Guan, J. Xu, Y. Zhang, Q. Liu, Y. Tian, S. Li, X. Qin, H. Yang, Y. Liu, *Biomaterials* **2019**, *205*, 106–119.
[39] X. Zhang, H. Li, C. Yi, G. Chen, Y. Li, Y. Zhou, G. Chen, Y. Li, Y. He, D. Yu, *Int. J. Nanomed.* **2020**, *15*, 9627–9638.
[40] Z. Ding, N. Luo, H. Yue, Y. Gao, G. Ma, W. Wei, *J. Mater. Chem. B* **2020**, *8*, 6845–6856.
[41] N. Luo, J. K. Weber, S. Wang, B. Luan, H. Yue, X. Xi, J. Du, Z. Yang, W. Wei, R. Zhou, G. Ma, *Nat. Commun.* **2017**, *8*, 14537.
[42] S. W. Lee, H. J. Park, L. Van Kaer, S. Hong, S. Hong, *Sci. Rep.* **2018**, *8*, 10081.
[43] J. Han, Y. S. Kim, M.-Y. Lim, H. Y. Kim, S. Kong, M. Kang, Y. W. Choo, J. H. Jun, S. Ryu, H.-y. Jeong, *ACS Nano* **2018**, *12*, 1959–1977.
[44] P. P. Wibroe, S. V. Petersen, N. Bovet, B. W. Laursen, S. M. Moghimi, *Biomaterials* **2016**, *78*, 20–26.

[45] C. Martín, A. Ruiz, S. Keshavan, G. Reina, D. Murera, Y. Nishina, B. Fadeel, A. Bianco, *Adv. Funct. Mater.* **2019**, *29*, 1901761.
[46] C. Martín, G. Jun, R. Schurhammer, G. Reina, P. Chen, A. Bianco, C. Ménard-Moyon, *Small* **2019**, *15*, 1905405.
[47] S. P. Mukherjee, A. R. Gliga, B. Lazzaretto, B. Brandner, M. Fielden, C. Vogt, L. Newman, A. F. Rodrigues, W. Shao, P. M. Fournier, M. S. Toprak, A. Star, K. Kostarelos, K. Bhattacharya, B. Fadeel, *Nanoscale* **2018**, *10*, 1180–1188.
[48] W. Tao, N. Kong, X. Ji, Y. Zhang, A. Sharma, J. Ouyang, B. Qi, J. Wang, N. Xie, C. Kang, H. Zhang, O. C. Farokhzad, J. S. Kim, *Chem. Soc. Rev.* **2019**, *48*, 2891–2912.
[49] H. Zhao, H. Chen, Z. Guo, W. Zhang, H. Yu, Z. Zhuang, H. Zhong, Z. Liu, *Chem. Eng. J.* ***2020****, 394, 124314.*
[50] H. T. Nguyen, J. H. Byeon, C. D. Phung, L. M. Pham, S. K. Ku, C. S. Yong, J. O. Kim, *ACS Appl. Mater. Interfaces* **2019**, *11*, 24959–24970.
[51] J. Ming, J. Zhang, Y. Shi, W. Yang, J. Li, D. Sun, S. Xiang, X. Chen, L. Chen, N. Zheng, *Nanoscale* **2020**, *12*, 3916–3930.
[52] X. Ji, N. Kong, J. Wang, W. Li, Y. Xiao, S. T. Gan, Y. Zhang, Y. Li, X. Song, Q. Xiong, S. Shi, Z. Li, W. Tao, H. Zhang, L. Mei, J. Shi, *Adv. Mater.* **2018**, *30*, 1803031.
[53] Y. Lin, Y. Wu, R. Wang, G. Tao, P.-F. Luo, X. Lin, G. Huang, J. Li, H.-H. Yang, *Chem. Commun.* **2018**, *54*, 8579–8582.
[54] M. Mahmoudi, N. Bertrand, H. Zope, O. C. Farokhzad, *Nano Today* **2016**, *11*, 817–832.
[55] P. C. Ke, S. Lin, W. J. Parak, T. P. Davis, F. Caruso, *ACS Nano* **2017**, *11*, 11773–11776.
[56] J. Mo, Q. Xie, W. Wei, J. Zhao, *Nat. Commun.* **2018**, *9*, 1–11.
[57] J. Mo, Y. Xu, X. Wang, W. Wei, J. Zhao, *Nanoscale* **2020**, *12*, 1742–1748.
[58] M. Han, L. Zhu, J. Mo, W. Wei, B. Yuan, J. Zhao, C. Cao, *ACS Appl. Bio Mater.* **2020**, *3*, 4220–4229.
[59] M. van Druenen, F. Davitt, T. Collins, C. Glynn, C. O'Dwyer, J. D. Holmes, G. Collins, *Langmuir* **2019**, *35*, 2172–2178.
[60] M. Naguib, M. Kurtoglu, V. Presser, J. Lu, J. Niu, M. Heon, L. Hultman, Y. Gogotsi, M. W. Barsoum, *Adv. Mater.* **2011**, *23*, 4248–4253.
[61] L. Bai, W. Yi, T. Sun, Y. Tian, P. Zhang, J. Si, X. Hou, J. Hou, *J. Mater. Chem. B* **2020**, *8*, 6402–6417.
[62] C. He, L. Yu, H. Yao, Y. Chen, Y. Hao, *Adv. Funct. Mater.* **2020**, 2006214.
[63] X. Li, J. Shan, W. Zhang, S. Su, L. Yuwen, L. Wang, *Small* **2017**, *13*, 1602660.
[64] J. Shi, J. Li, Y. Wang, J. Cheng, C. Y. Zhang, *J. Mater. Chem. B* **2020**, *8*, 5793–5807.
[65] Q. Han, X. Wang, X. Jia, S. Cai, W. Liang, Y. Qin, R. Yang, C. Wang, *Nanoscale* **2017**, *9*, 5927–5934.
[66] F. Jiang, B. Ding, S. Liang, Y. Zhao, Z. Cheng, B. Xing, P. a. Ma, J. Lin, *Biomaterials* **2021**, *268*, 120545.
[67] D. Zhang, P. Cui, Z. Dai, B. Yang, X. Yao, Q. Liu, Z. Hu, X. Zheng, *Nanoscale* **2019**, *11*, 19912–19922.
[68] L. He, T. Nie, X. Xia, T. Liu, Y. Huang, X. Wang, T. Chen, *Adv. Funct. Mater.* **2019**, *29*, 1901240.
[69] X. Dong, R. Cheng, S. Zhu, H. Liu, R. Zhou, C. Zhang, K. Chen, L. Mei, C. Wang, C. Su, X. Liu, Z. Gu, Y. Zhao, *ACS Nano* **2020**, *14*, 5400–5416.
[70] L. Deng, X. Pan, Y. Zhang, S. Sun, L. Lv, L. Gao, P. Ma, H. Ai, Q. Zhou, X. Wang, *Int. J. Nanomed.* **2020**, *15*, 2971.
[71] D. Baimanov, J. Wu, R. Chu, R. Cai, B. Wang, M. Cao, Y. Tao, J. Liu, M. Guo, J. Wang, *ACS Nano* **2020**, *14*, 5529–5542.
[72] Z. Gu, S. H. Chen, Z. Ding, W. Song, W. Wei, S. Liu, G. Ma, R. Zhou, *Nanoscale* **2019**, *11*, 22293–22304.
[73] Z. Miao, D. Huang, Y. Wang, W.-J. Li, L. Fan, J. Wang, Y. Ma, Q. Zhao, Z. Zha, *Adv. Funct. Mater.* **2020**, *30*, 2001593.
[74] Q. He, H. Hu, Q. Zhang, T. Wu, Y. Zhang, K. Li, C. Shi, *Chem. Eng. J.* **2020**, 125478.
[75] Y. Liu, Y. Pan, W. Cao, F. Xia, B. Liu, J. Niu, G. Alfranca, X. Sun, L. Ma, J. M. de la Fuente, J. Song, J. Ni, D. Cui, *Theranostics* **2019**, *9*, 6867–6884.
[76] F. Gong, M. Chen, N. Yang, Z. Dong, L. Tian, Y. Hao, M. Zhuo, Z. Liu, Q. Chen, L. Cheng, *Adv. Funct. Mater.* **2020**, *30*, 2002753.
[77] K. Ni, T. Luo, G. T. Nash, W. Lin, *Accounts Chem. Res.* **2020**, *53*, 1739–1748.
[78] G. Chong, J. Zang, Y. Han, R. Su, N. Weeranoppanant, H. Dong, Y. Li, *Nano Res.* **2021**, *14*, 1244–1259.
[79] K. Ni, T. Luo, G. Lan, A. Culbert, Y. Song, T. Wu, X. Jiang, W. Lin, *Angew. Chem. Int. Ed.* **2020**, *132*, 1124–1128.
[80] K. Ni, T. Aung, S. Li, N. Fatuzzo, X. Liang, W. Lin, *Chem* **2019**, *5*, 1892–1913.
[81] B. Ma, S. Wang, F. Liu, S. Zhang, J. Duan, Z. Li, Y. Kong, Y. Sang, H. Liu, W. Bu, L. Li, *J. Am. Chem. Soc.* **2019**, *141*, 849–857.
[82] K. Lu, C. He, W. Lin, *J. Am. Chem. Soc.* **2014**, *136*, 16712–16715.
[83] K. Lu, C. He, N. Guo, C. Chan, K. Ni, G. Lan, H. Tang, C. Pelizzari, Y.-X. Fu, M. T. Spiotto, *Nat.*

Biomed. Eng. **2018**, *2*, 600–610.
[84] K. Ni, T. Luo, A. Culbert, M. Kaufmann, X. Jiang, W. Lin, *J. Am. Chem. Soc.* **2020**, *142*, 12579–12584.
[85] K. Ni, G. Lan, Y. Song, Z. Hao, W. Lin, *Chem. Sci.* **2020**, *11*, 7641–7653
[86] X. Long, Z. Wang, S. Xiao, Y. An, S. Yang, *Mater. Today* **2016**, *19*, 213–226.
[87] Z. Cao, B. Li, L. Sun, L. Li, Z. P. Xu, Z. Gu, *Small Methods* **2020**, *4*, 1900343.
[88] L. Yan, S. Gonca, G. Zhu, W. Zhang, X. Chen, *J. Mater. Chem. B* **2019**, *7*, 5583–5601.
[89] S. Yan, B. E. Rolfe, B. Zhang, Y. H. Mohammed, W. Gu, Z. P. Xu, *Biomaterials* **2014**, *35*, 9508–9516.
[90] N. Wang, Z. Wang, Z. Xu, X. Chen, G. Zhu, *Angew. Chem. Int. Ed.* **2018**, *57*, 3426–3430.
[91] S. Gan, X. Tong, Y. Zhang, J. Wu, Y. Hu, A. Yuan, *Adv. Funct. Mater.* **2019**, *29*, 1902757.
[92] S. Mura, J. Nicolas, P. Couvreur, *Nat. Mater.* **2013**, *12*, 991–1003.
[93] T. Xia, C. Lei, C. Xu, N. Peng, Y. Li, X.-Y. Yang, Z.-Z. Cheng, M. Gauthier, H.-Z. Gu, T. Zou, *Langmuir* **2020**, *36*, 14268–14275.
[94] T. Li, M. Peng, Z. Yang, X. Zhou, Y. Deng, C. Jiang, M. Xiao, J. Wang, *Acta Biomater.* **2018**, *71*, 96–107.
[95] K. L. Spiller, S. Nassiri, C. E. Witherel, R. R. Anfang, J. Ng, K. R. Nakazawa, T. Yu, G. Vunjak-Novakovic, *Biomaterials* **2015**, *37*, 194–207.
[96] Y. Niu, Z. Wang, Y. Shi, L. Dong, C. Wang, *Bioact. Mater.* **2021**, *6*, 244–261.
[97] S. Wang, H. Zheng, L. Zhou, F. Cheng, Z. Liu, H. Zhang, L. Wang, Q. Zhang, *Nano Lett.* **2020**, *20*, 5149–5158.
[98] H. Huang, W. Feng, Y. Chen, J. Shi, *Nano Today* **2020**, *35*, 100972.

Graphical Abstract

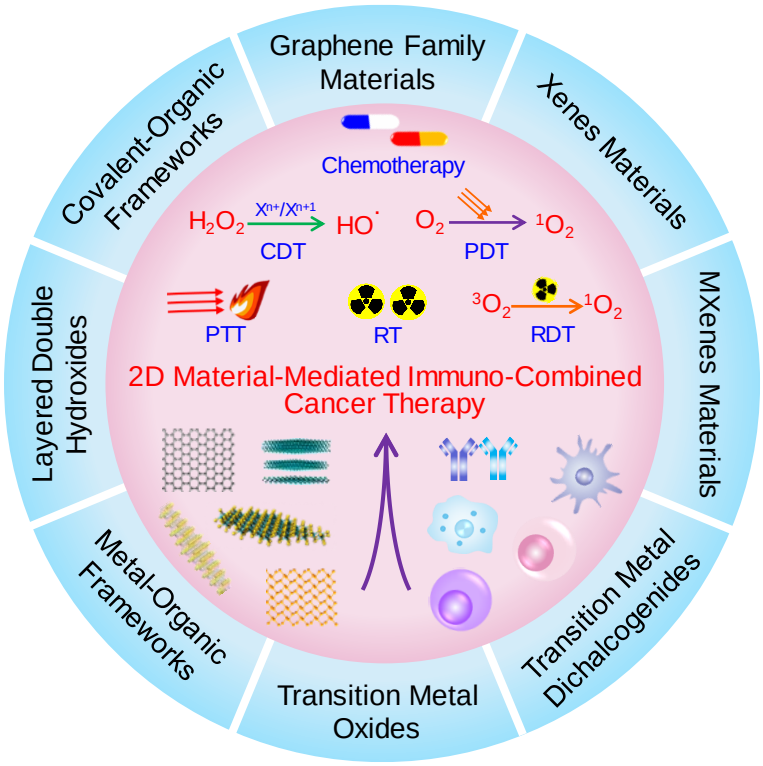

This Review focuses on the recent development of 2D material-mediated immune combined cancer therapy, and aims to understand the synergistic effect between immune response and other therapeutic strategies. These synergistic approaches intend to go beyond the classical strategies based on a simple delivery function of immune modulators by nanomaterials. Further, the effects of the 2D materials themselves and their surface properties on the induction of an immune response will be also discussed.

Biographies

Alberto Bianco

Dr. Alberto Bianco received his PhD in 1996 from the University of Padova. As a visiting scientist, he worked at the University of Lausanne, the University of Tübingen (as an Alexander von Humboldt fellow), the University of Padova and Kyoto University. He is currently Research Director at the CNRS in Strasbourg. His research interests focus on the design of multifunctional carbon-based nanomaterials for therapy, diagnostics and imaging. He has been recently elected Fellow of the European Academy of Science and of the Academia Europaea, and in 2019 he obtained the CNRS Silver Medal. Since 2011 he is Editor of the journal CARBON.

Baojin Ma

Dr. Baojin Ma received his PhD in 2019 from Shandong University. During 2019-2021, he worked as a postdoctoral fellow in Dr. A. Bianco's group at the CNRS in Strasbourg (France). He is currently research Professor in the School and Hospital of Stomatology at Shandong University. His research interests include the design and synthesis of multifunctional biomaterials for cancer therapy and tissue repair.